Nonequilibirum Assembly, Retroviruses, and Conical Structures

Artem Levandovsky and Roya Zandi

Department of Physics, University of California, Riverside California 92521, USA

(Received 15 January 2009; published 13 May 2009)

We study the spontaneous assembly of viral shells composed of several identical subunits under nonequilibrium conditions. We find that within the basic continuum elasticity framework, the nonequilibrium assembly process is able to predict the formation of structures pertinent to retroviruses. Our minimal model of assembly yields a unified one-dimensional phase diagram in which the appearance of spherical, irregular, conical and cylindrical structures of retroviruses is seen to be governed by the spontaneous curvature of protein subunits.

DOI: 10.1103/PhysRevLett.102.198102 PACS numbers: 87.16.Gj, 81.16.Dn

In recent years, there have been several studies aimed at understanding the physical principles governing the formation of viral particles for both their material and biological applications [1–6]. The assembly of retroviruses has been, in particular, receiving additional attention due to their oncogenic activity and the fact that human immunodeficiency virus (HIV) is connected to the AIDS pandemic. Retroviruses, like all other viruses, contain a proteineous shell (or capsid) that encloses viral genetic material. While most viral capsids are spherical and adopt structures with icosahedral symmetry with a well-defined size (T number), polymorphism is common among retroviral capsids. For example, recent studies show that the capsid of Rous sarcoma virus (RSV), a well-studied avian retrovirus, adopts spherical, tubular, and irregular polyhedral structures [7,8]. In the case of HIV, capsid proteins self-assemble predominantly into conical structures but cylindrical and other irregular shapes have also been observed [9]. Despite significant variations, retroviral capsids of different genera appear to be composed of a two-dimensional hexagonal lattice (embedded in 3D space) with 12 disclinations (pentagons).

It is remarkable that under special formation conditions mature HIV capsids will readily self-assemble from their isolated capsid protein and nucleic acid components. The spontaneous formation of conical structures is the distinguishable feature of mature HIV capsids, which gives rise to a number of important physical questions. Does spontaneous curvature determine the shape of the viral capsids? Do kinetics rather than thermodynamics determine the final structure of capsids? Does RNA play an active role in the final structure of capsids?

Ganser *et al.* [10] recently performed a series of *in vitro* experiments with 1400-nucleotide HIV-1 RNA and a pure recombinant CA-NC fusion protein and observed that a mixture of cones and cylinders form under physiological conditions. To elucidate the role of genome in HIV assembly, they investigated the effect of 6400-nt RNA from tobacco mosaic virus and 1400-nt fragment from the bacillus stearothermophilus 16S ribosomal RNA in the formation of conical shells [10]. All these experiments indicated that neither size nor a specific RNA sequence affect the asymmetry observed in cones. In fact, at high (0.5 M) salt concentrations, in the absence of RNA, hollow cylinders and cones also assembled confirming that a genome template is not required for cone formation.

Continuum elasticity theory has been recently applied to investigate the conical structure of mature HIV capsids [11]. According to these equilibrium studies, the conical capsids do not constitute energy minimum structures unless their volume and height are fixed. The volume occupied by the encapsidated genome or surrounding lipid membrane has been suggested as physical constraints present during assembly. More recently, Hicks and Henley [6] have investigated the irreversible growth of viral shells using elasticity theory. Their studies report the formation of highly irregular structures but the occurrence of conical shapes resembling experimentally observed HIV cones remains unexplained.

There have been a number of experiments indicating viral shells behave like elastic objects. Indeed, continuum elasticity has successfully explained the shape transition from spherical to sharply faceted capsids [1] as well as force-deformation curves measured in atomic force microscopy (AFM) experiments [3,4]. In this Letter we apply continuum elasticity theory to study the growth of viral capsids under nonequilibrium conditions. We find that spontaneous curvature, the preferred angle between protein subunits, has a key role in determining the structure of retroviral capsids, see Fig. 1. According to our studies, the specific form of conical HIV shells is not induced by a complex biological mechanism (such as the presence of a template or the influence of a surrounding membrane) but rather it is the natural response of an elastic sheet growing under simple rules of nonequilibrium assembly. Our findings are consistent with the experimental studies of Wright *et al.* [12] as well as Erlich *et al.* [13], which emphasize the importance of spontaneous curvature during HIV assembly.

In our model, the nonequilibrium assembly of viral shells includes two essential steps: (i) addition of subunits

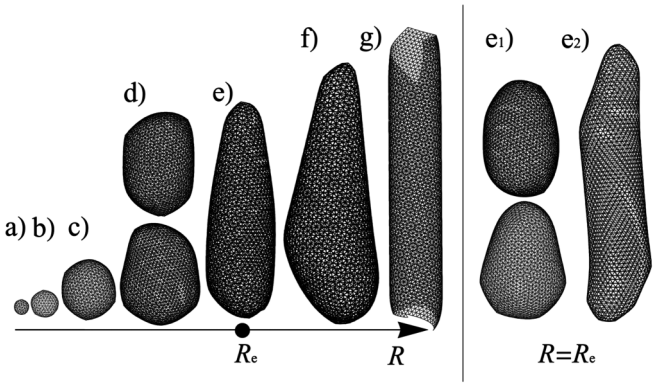

FIG. 1. Structures produced by our numerical simulations. Left: Shape and relative size of viral structures vs the spontaneous radius of curvature, R, which is determined by the quantity Δ in Fig. 2. Here $a_0 = 1$ and Δ is (a) 0.2, (b) 0.15, (c) 0.1, (d) 0.08, (e) 0.076, (f) 0.075, and (g) 0.072. Right: Distribution of shapes around the deterministic structure (e) if 0.5% of deterministic steps in the growth process is made random (see the text). Structures in (e), (e1), and (e2) have the same spontaneous radius of curvature, R_e, corresponding to $\Delta = 0.076$. Both (d) and (e1) correspond to one structure each in two different views (bottom and top).

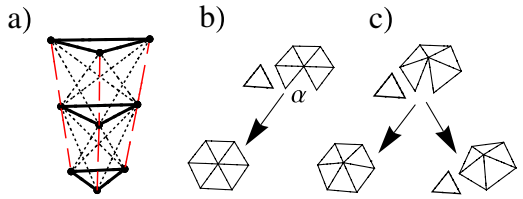

FIG. 2 (color online). (a) The unit cell of the model in the form of a triangular prism. The solid lines represent springs with spring constant k_1. The equilibrium lengths of springs in three layers (from top to bottom) are $a_0 + 2\Delta$, a_0 and $a_0 - 2\Delta$. Three layers are connected by springs in the vertical direction noted by dashed red lines (spring constant k_2 and equilibrium length of a_0) and also by additional springs noted by dotted lines with spring constant k_3. The choice of $k_2 = k_1/2$ and $k_3 = k_1/3$ makes the system elastically isotropic. The effect of spontaneous curvature is achieved by making the top triangle (solid line triangle) slightly larger than the bottom triangle (i.e., $\Delta \neq 0$). (b) For a flat plate (zero spontaneous curvature) the opening angle of five units is exactly 60 deg. and only hexagons are formed. However, in the presence of spontaneous curvature, (c) the opening angle α is always less than 60 deg., and therefore a newly added triangle has to be compressed to form a hexagon or the five existing triangles need to be stretched to form a pentagon.

into the growing shell and (ii) elastic relaxation of the partially formed structure. We model the protein subunits as triangular prisms made of point masses arranged in three layers as illustrated in Fig. 2(a). The parameter Δ (see caption of Fig. 2) determines the radius of curvature of the outer shell as $R = a_0(1 + a_0/2\Delta)$. The system of point masses connected by harmonic springs with spring constants k_m and equilibrium lengths a_m is described by

$$H = \frac{1}{2} k_m (|r_j - r_j| - a_m)^2. \quad (1)$$

The coefficients k_m are selected such that in the continuum limit the system has the isotropic elasticity of materials with equal Lame coefficients as in Ref. [1] (the Poisson ratio of such material is $1/3$ for 2D and $1/4$ for 3D systems). The details of this 3D Hamiltonian and its advantages over 2D models in representing the viral shells will be discussed elsewhere [14]. Here we focus on describing the process of shell growth and the underlying physical principles resulting in formation of different structures observed in the capsids of retroviruses.

Several studies indicate that the attractive interaction between protein subunits forming mature HIV capsids is weak. Therefore, we assume that the growth process is so slow that each subunit at the growing edge has enough time to diffuse along it, explore the energy landscape, and attach itself to a place in which the subunit maximizes the number of intermolecular bonds. This, in fact, corresponds to a location at the growing edge with a minimum opening angle α, see Fig. 2(b). We consider the deterministic growth where attachment of each new unit cell happens in the most probable place determined by the value of the opening angle (if there are equivalent positions at the edge, then one of them will be randomly chosen). Our criteria for formation of pentagons and hexagons is illustrated in Figs. 2(b) and 2(c). All-atomistic simulations are needed to provide a precise rule for formation of hexagons or pentagons. In the absence of such simulations, we adopt a phenomenological approach similar to the one employed in problems of crack propagation [15] (another problem with moving boundaries), where the critical value of a strain is used as a criterion for crack growth. In this work in a similar fashion we define a critical value for the opening angle, α. For the structures presented here, we chose the critical value to be $\alpha = 30$ deg. While the edges of an opening angle below 30 deg. merge to form a pentagon, a new triangle will be added to an opening angle between 30 and 60 deg. to create a hexagon. As in problems of crack propagation, the results are not very sensitive to the exact value of the critical opening angle α so our conclusion presented below is found to be robust.

After each attachment or merging step, using the Verlet algorithm we integrate the equations of motion obtained from Eq. (1) for all nodes to achieve the relaxed overdamped configuration of a partially formed elastic shell. This process is followed by the addition of another subunit to the growing edge. We note that in the nonequilibrium process considered here, once a pentamer or hexamer is formed it can no longer dissociate. Our algorithm follows the locally minimum energy path, which, under many conditions that lead to productive assembly, is reasonably close to the most probable assembly pathways and hence yields a meaningful representation of the final capsid structures.

An additional step is performed when in the process of growth two topologically distant parts of edge become close to each other to the point that they are less than one lattice spacing apart. A short-ranged Morse potential mimicking the hydrophobic attraction between the protein subunits, which are distant along the edge, ensures the closure of the surface, as is illustrated in Figs. 3(g) and 3(h). Note also that as soon as two distant parts of a structure come close to each other, they merge and thus the excluded volume interaction is never violated in our structures.

The results of our numerical analysis are presented in Fig. 1 in the form of a phase diagram of generic shapes resulting from the nonequilibrium assembly of elastic shells versus spontaneous radius of curvature. The number of subunits in Fig. 1 changes from a hundred to a few thousands [about 2300 for the cone in Fig. 1(f)]. As shown in the figure, with increasing radius of curvature the shell size also increases as expected. This general trend is modulated by a deviation from spherical shape as one proceeds from the smaller radius of curvature to the larger ones, Figs. 1(e) and 1(f). On the left side of Fig. 1, the dominant shapes are rather spherical, which is the consequence of the formation of pentagons soon after the growth process begins. In general, the larger spontaneous curvature promotes smaller opening angles and consequently facilitates the creation of pentagons. The distances between pentagons in Figs. 1(a) and 1(b) is almost uniform

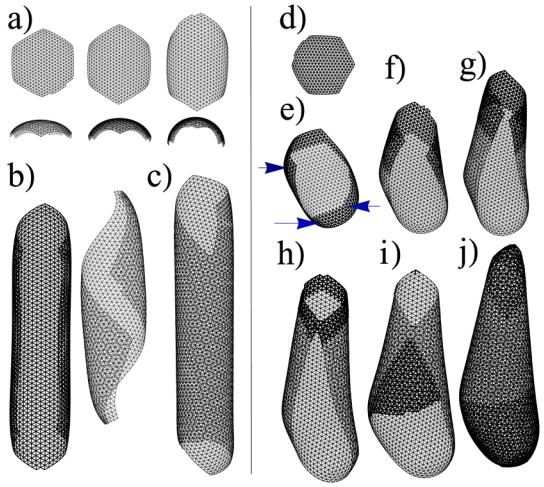

FIG. 3 (color online). Left: (a) Snapshots of the early stages of a tube growth in two different projections. As the capsid grows, the hexagonal symmetry of the shell transforms into a rectangular one. (b) Rectangular sheets grow and wrap into (c) cylindrical tubes. The orientation of the hexagonal lattice with respect to the cylinder axis depends on the way rectangular sheets fold into cylindrical structures. Right: Snapshots of formation of the conical structures of Fig. 1(f). Darker color indicates most recent accretion. Early stages of growth in (d) is similar to those for cylindrical tubes in (a). In part (e) three pentagons are formed (indicated by arrows). (f) Pentagons make the structure less symmetrical compared to (b). The remainder of pentagons appear only in final stages of growth.

but not identical. Note that we do not observe icosahedral structures in our work, which is focused on large shells. Many studies indicate that the presence of scaffold proteins is necessary for the formation of large icosahedral shells.

In Fig. 1(g), we observe well-defined cylindrical shapes, which contain no pentagons. The small spontaneous curvature between the protein subunits makes the formation of pentagons energetically costly, keeping the opening angle α (see Fig. 2) at values just slightly below 60 deg. The initial stage of assembly of a cylindrical shell is depicted in Fig. 3(a). At the early stages of growth, the shell can be described as a spherical cap growing in six directions with approximately the same speed. As the growth proceeds, at some point it becomes impossible to construct a spherical surface out of hexagons without a large cost of energetic distortions. A spherical cap can be built out of triangular subunits only if the size of the cap is small (i.e., when distortions are minute). As the size of the shell increases, it adopts nonspherical structures that minimize the distortions (for a review of distortion appearing in the mapping of a flat plane to a sphere see, e.g., [16,17]). To this end, the cap illustrated in Fig. 3(a) will grow such that two of its sides become flatter than the other four. This modifies the growth speed in each direction, making the shell grow faster in the vertical direction [Fig. 3(a)], and thus a hexagonal sheet curved in the form of spherical cap transforms into a curved rectangular sheet. Rectangular sheets with various aspect ratios of length to width produce tubes with different chiral vectors, Fig. 3(b). Consistent with *in vitro* studies [7,10], tubes are open at both ends, Fig. 3(c).

As shown above, depending on the spontaneous curvature the viral shells can assume structures with spherical or cylindrical symmetries. An interesting question now arises, what other shapes can the shells adopt if the spontaneous curvature is between these two extreme limits? In the phase diagram of Fig. 1, there are two distinguishable states between cylindrical and spherical structures. One of these two states, Fig. 1(d), is characterized by a large degree of shape irregularity and also has already been observed in Ref. [6]. In Fig. 1(d) the distance between the pentamers assembled at the initial stages of the growth is considerably larger than that formed in spherical viruses [Figs. 1(a)–1(c)]. The variation of distances between neighboring pentagons often leads to irregular shapes that avoid simple classification. Figures 1(d) and 1(e1) illustrate two different 2D views of two different irregular structures. Depending on the angle of view, the same shell can be classified as having a conical [bottom] or a cylindrical [top] structure. Theoretical documentation of such ambiguity is very important for experimental studies in which 3D shape distributions are deduced from 2D measurements of shape projections. The large shape variations of this state may have complicated the previous nonequilibrium studies investigating the elusive conical shape of mature HIV viruses.

The other state in the sphere-cylinder transition diagram, Figs. 1(e) and 1(f) , corresponds to the structures that

strikingly resemble the experimentally observed conical shapes for HIV viruses [9]. The right panel in Fig. 3 illustrates the process by which conical structures form. The hexagonal shell in Fig. 3(d) has the same symmetry as the one presented in Fig. 3(a) which assembles later into a cylindrical structure. However, shortly after destruction of hexagonal symmetry in this case, a small number of pentagons form and the resulting sheet wraps into slightly distorted tubes that later in the process of growth can be identified as conical structures, Fig. 3(j).

At the moment, there is no consensus as to how a conical capsid grows in vitro. Briggs *et al.* [18] suggest a template-assisted scheme in which each cone starts to form from the narrow tip while Benjamin *et al.* [9] suggest the opposite trend with the base of a cone forming first and the narrow tip last. The latter is based on measurements indicating that the tip is likely to have an imperfection in the form of a small opening (hole). We believe that the study performed here provides an understanding of how a viral shell grows. Note that while protein-genome interaction and/or a surrounding membrane can help the formation of conical structures, according to our results their presence is not necessary for the process. As indicated in Figs. 3(d)–3(j), the assembly begins with the formation of a large hexagonal sheet with pentagons formed later on due to strain accumulated in the sheet. We note that the experimentally observed holes at the tip of a cone sometimes appear in our simulations as well. A large concentration of strain at the cone tip might prevent the closure of the hole since only limited deformation of subunits is allowed.

The phase diagram presented in Fig. 1 is unique in that all basic shapes (spherical, irregular, conical, and cylindrical) appear as a consecutive series of structures governed by the spontaneous curvature of protein subunits with no constraint on area or volume of the structure. Unlike the first-order phase transition suggested in previous studies [11] based on equilibrium statistical mechanics and assembly constraints, the transition we observe in nonequilibrium self-assembly of retroviruses is not first-order but rather goes through the formation of two intermediary states corresponding to irregular and conical structures.

The structures presented in the phase diagram in the left panel of Fig. 1 is obtained deterministically; however, in experiments one will always observe a distribution of shapes around the deterministic configurations. To facilitate comparison with experiments, we construct structures in Figs. 1(e), 1(e1), and 1(e2) such that have the same spontaneous radius of curvature, $R = R_e$. Structure 1(e) is formed as explained before but structures 1(e1) and 1(e2) are obtained when a small percentage (0.5%) of subunits were added at random positions at the growing edge whereas the rest (99.5%) were placed according to the deterministic procedures described above. The resulting structures can be recognized as shapes pertinent to mature HIV viruses reported in the experiments of Ref. [9].

In summary, our model predicts that the shapes of retroviruses can be explained by the dynamics of formation of pentagons. For the small spontaneous radii of curvature, the pentagons can assemble almost uniformly in the vicinity of each other to form spheroidal shapes. Larger radii of curvature delay assembly of pentagons and a large group of hexagons tend to wrap into cylindrical shapes. We identify the conical shape of HIV as an intermediate state in the sphere-to-cylinder transition. Our studies show that even within one class of shapes (e.g., cones) the introduction of pentamers into different positions in a hexameric lattice causes one cone to differ from another. This is indeed one of the major challenges facing the structural virologist investigating mature HIV since each HIV capsid is unique; i.e., it has a different size and a different number of subunits [12]. To test several concepts presented in this Letter, it would be interesting to carry out a set of systematic assembly studies with various mutated proteins that have different spontaneous curvatures and construct an experimental phase diagram similar to the one shown in Fig. 1.

The authors would like to acknowledge helpful discussions with B. Ganser, W. M. Gelbart, and L. Pryadko. This work is supported by NSF Grant No. DMR-06-45668.

[1] J. Lidmar *et al.*, Phys. Rev. E **68**, 051910 (2003).
[2] M. F. Hagan, Phys. Rev. E **77**, 051904 (2008); A. Šiber and R. Podgornik, Phys. Rev. E **76**, 061906 (2007); D. C. Rapaport, Phys. Rev. Lett. **101**, 186101 (2008); H. D. Nguyen and C. L. Brooks III, Nano Lett. **8**, 4574 (2008); T. Keef, A. Taormina, and R. Twarock, Phys. Biol. **2**, 175 (2005).
[3] E. Nurmemmedov *et al.*, Q. Rev. Biophys. **40**, 327 (2007).
[4] J. P. Michel *et al.*, Proc. Natl. Acad. Sci. U.S.A. **103**, 6184 (2006).
[5] R. Zandi *et al.*, Proc. Natl. Acad. Sci. U.S.A. **101**, 15 556 (2004).
[6] S. D. Hicks and C. L. Henley, Phys. Rev. E **74**, 031912 (2006).
[7] K. Mayo *et al.*, J. Mol. Biol. **325**, 225 (2003).
[8] J. B. Heymann *et al.*, Comput. Math. Methods Med. **9**, 197 (2008).
[9] J. Benjamin *et al.*, J. Mol. Biol. **346**, 577 (2005).
[10] B. K. Ganser *et al.*, Science **283**, 80 (1999).
[11] T. T. Nguyen *et al.*, Phys. Rev. Lett. **96**, 078102 (2006); Phys. Rev. E **72**, 051923 (2005).
[12] E. R. Wright *et al.*, EMBO J. **26**, 2218 (2007).
[13] L. S. Ehrlich *et al.*, Biophys. J. **81**, 586 (2001).
[14] A. Levandovsky and R. Zandi (unpublished).
[15] T. Martin *et al.*, Phys. Rev. E **71**, 036202 (2005).
[16] K. F. Gauss, *General Investigations of Curved Surfaces* (Dover Publications, New York, 2005).
[17] J. Brainerd and A. Pang, Comput. Geosci. **27**, 299 (2001).
[18] J. A. G. Briggs *et al.*, Structure **14**, 15 (2006).